The influence of the microstructure of high noble gold-platinum dental alloys on their corrosion and biocompatibility in vitro

M. Colic[1,2], D. Stamenkovic[3], I. Anzel[4], G. Lojen[4], R. Rudolf[4],*

[1] Institute of Medical Research, Military Medical Academy, Belgrade, Serbia; [2] Medical Faculty, University of Nis, Nis, Serbia; [3] Faculty of Stomatology, University of Belgrade, Belgrade, Serbia, [4] Faculty of Mechanical Engineering, University of Maribor, Maribor, Slovenia

* Corresponding author:
Rebeka Rudolf, University of Maribor, Faculty of Mechanical Engineering, Smetanova ulica 17, 2000 Maribor, Slovenia,
e-mail: rebeka.rudolf@uni-mb.si

Abstract

The aim of this work was to compare the microstructures of two high noble experimental Au-Pt alloys with similar composition with their corrosion and biocompatibility in vitro. We showed that Au-Pt II alloy, composed of 87.3 wt.% Au, 9.9 wt.% Pt, 1.7 wt.% Zn and 0.5 wt.% Ir + Rh + In, although possessing better mechanical properties than the Au-Pt I alloy (86.9 wt.% Au, 10.4 wt.% Pt, 1.5 wt.% Zn and 0.5 wt.% Ir + Rh + In), exerted higher adverse effects on the viability of L929 cells and the suppression of rat thymocyte functions, such as proliferation activity, the production of Interleukin-2 (IL-2), expression of IL-2 receptor and activation – induced apoptosis after stimulation of the cells with Concanavalin-A. These results correlated with the higher release of Zn ions in the culture medium. As Zn^{2+}, at the concentrations which were detected in the alloy's culture media, showed a lesser cytotoxic effect than the Au-Pt conditioning media, we concluded that Zn is probably not the only element responsible for alloy cytotoxicity. Microstructural characterization of the alloys, performed by means of scanning electron microscopy in addition to energy dispersive X-ray and X-ray diffraction analyses, showed that Au-Pt I is a two-phase alloy containing a dominant Au-rich α_1 phase and a minor Pt-rich α_2 phase. On the other hand, the Au-Pt II alloy additionally contained three minor phases: $AuZn_3$, Pt_3Zn and $Au_{1.4}Zn_{0.52}$. The highest content of Zn was identified in the Pt_3Zn phase. After conditioning, the Pt_3Zn and $AuZn_3$ phases disappeared, suggesting that they are predominantly responsible for Zn loss, lower corrosion stability and subsequent lower biocompatibility of the Au-Pt II alloy.

Key words: Au-Pt alloy, biocompatibility, corrosion, Zn, microstructure

1 Introduction

Gold alloys are used in dentistry, not only for their preferred golden colour, but also because they maintain an extremely high chemical stability in the mouth. They also possess several desirable mechanical properties such as high strength, ductility and elasticity (1).

From among the various types of alloys used for porcelain fused to metal (PFM) restorations, Au-Pt based high noble alloys have had the advantage of being around for some considerable time. They are part of clinical experience and are extremely successful (2). The bond between the ceramic and the metal is particularly strong and highly reliable. When considering the formulations of Au-Pt-based high noble alloys for porcelain bonding (3), high Au contents are required to ensure biocompatibility, and large Pt concentrations are necessary to raise the melting range sufficiently above the porcelain firing temperature to prevent distortion during porcelain application (2,3). The addition of Zn lowers the liquid alloy's surface tension, thus enabling the material to be cast into very thin sections. Zn also serves as a dezoxidant and together with Ir and In protect other metals from oxidation. Micro-alloying metals are also added to form a thin oxide film on the alloy's surface during the porcelain firing cycle, as a grain refiner (Ir), to promote bonding between the alloy and the ceramic (In) while the presence of Rh enhances both strength and colour (3-5).

High Au-content dental alloys, including Au-Pt alloys, show good biocompatibility due to the corrosion resistance of high noble elements (6-7). However, in vitro studies have demonstrated the release of microalloying elements from these alloys in culture media, artificial saliva or distilled water (6-10). Some of them, especially Zn and Cu, could reach levels that cause the detectable cytotoxic effect (6,8,9). Metal corrosion depends on an alloy's composition and microstructure, biomechanical conditions, mode of casting and polishing, composition and electrolyte characteristics of solutions used for alloy conditioning, size of the alloy's surface area exposed to solutions, duration of incubation time, and many other factors (6-10).

We prepared two experimental Au-Pt alloys with similar compositions (11). The slightly higher Zn content by 0.2 wt. % in the Au-Pt II alloy was chosen to improve bonding strength between porcelain and alloy, and mechanical properties for the tooth's metallic substitute. The coefficients of thermal expansion were 14.55 x 10^{-6} / °C (Au-Pt I) and 14.50 x 10^{-6} / °C (Au-Pt II).

Our preliminary viability study on L929 cells showed that Au-Pt I and Au-Pt II alloys, in spite of their similar composition, significantly differed in their biocompatibility. We hypothesized that differences in microstructure and distribution of microalloying elements within phases, especially Zn, are responsible for the alloy's corrosion properties and subsequent cytotoxicity of the alloy conditioning media. To test this hypothesis the aim of this study was: 1. to evaluate metal ion release from Au-Pt I and Au-Pt II alloys into the culture media; 2. to investigate the cytotoxic effect of Au-Pt conditioning media, using a standard viability assay, on L929 cells and more sensitive T-cell function and apoptosis assays; 3. to check whether the released Zn ions in the conditioning media cause the same biological activity as exogenous added Zn; 4. to compare the microstructure of the alloys before and after conditioning, in order to identify those phases and microelements responsible for the alloy's corrosion behaviour.

2 Material and methods

2.1 Production of Au-Pt alloys

The production of Au-Pt alloys was described in detail in our previous publications (11). Briefly, the melting of very pure components (Au= 99.99 wt.%, Pt= 99.99 wt.%, Zn= 99.99 wt.%, In= 99.99 wt.%, Rh in the form of PtRh (90:10)= 99,99 wt.%, and Pt in the form of PtIr (90:10)= 99.99 wt.%) was performed in a vacuum induction melting furnace at vacuum p = 10^{-3} mbar and temperature T=1600°C. The casting of both melted alloys was performed at argon pressure above 1,03 bar in a metal cast of 8 mm diameter and was followed by subsequent thermo-mechanical treatment (procedures of profile and polish milling, thermal treatments) and cutting off a strip to regulate the shape (plate thickness 2 mm) (11). During production of the experimental Au-Pt I alloy, some small variations in the production stages were carried-out when compared to producing the Au-Pt II alloy, but the basic principles were the same for both alloys.

The composition of the alloys (wt. %) was as follows: Au-Pt I (Au - 86.9; Pt – 10.4; Zn – 1.5; Ir – 0.2; Rh – 0.2; In – 0.1); Au-Pt II (Au - 87.3; Pt – 9.9; Zn – 1.7; Ir – 0.2; Rh – 0.2; In – 0.1).

2.2 Preparation of Au-Pt alloy samples for biocompatibility testing

Samples of both Au-Pt alloys were cast as discs (diameter 10 mm, height 1 mm). Casting involved a conventional lost-wax technique which stimulates the preparation of cast metal alloy for clinical use. Wax specimens were placed into phosphate-bonded investments and heated in a ZC Aurodent furnace, type 2206A, at 850°C. The alloys were melted in a glass-graphite crucible and cast, after wax elimination, in the vacuum, using a Manfredi high-frequency induction casting machine at 1280°C. After cooling, the specimens were sandblasted with 250μ Al_2O_3. Polishing was performed using stone burrs as described (8).

The discs were soaked in a detergent (Herba, Parafarm, Subotica, Serbia) for 5 minutes and then scrubbed using a soft bristle brush and rinsed in tap water for 10 mins. After cleaning by sonification (twice for 5 mins in distilled water) and once in ethanol (5 mins), and then dried at room temperature, the specimens were autoclaved at a temperature of 180°C for 2 hours.

2.3 Extraction procedure and analysis of element release

The extraction procedure included the cultivation of 3 Au-Pt I and Au-Pt II alloy disks in 35 mm-diameter Petri dishes with 3 ml of complete culture medium composed of RPMI-1640 medium (Sigma, Munich, Germany) with the addition of 10% fetal calf serum (FCS) (ICN – Costa Mesa) and antibiotics (Galenika, Zemun, Serbia), including gentamycin (10 μg/ml), penicillin (100 units / ml) and streptomycin (125 μg/ml) for 14 days (relative surface area 1.88 cm^2/ml medium) in an incubator (Flow, Irvine, Scotland) with 5% CO_2 at 37°C. After that, media were collected and kept at +4°C. The same procedure was repeated twice by incubating the alloys with fresh media. At the end of the 42-day procedure, conditioning media were collected and pooled. The control conditioning medium was a complete RPMI medium incubated without alloys. Media were used for chemical analysis and biological testing.

The concentrations of metal ions in the pooled conditioning media were performed by Inductively Coupled Plasma Atomic Emission Spectrophotometry (ICP-AES) (Perken-Elmer). Triplicate absorbance readings per element were recorded for each sample.

2.4 Cytotoxicity testing

The cytotoxicity of the Au-Pt - conditioning media and $ZnCl_2$ was tested using a standard method for measurement of mitochondrial succinic dehydrogenase (SDH) activity in L929 mouse fibroblasts. Cells were routinely cultivated in the complete RPMI medium.

L929 cells were cultivated in 96-well plates (ICN) (0.4x10^4 cells/well) with conditioning alloy media, control conditioning medium, fresh culture medium or different concentrations of $ZnCl_2$ (Fluka) dissolved in a fresh complete RPMI medium. The cells were plated in 6-plikates in a volume of 200 μl of medium. After a 3-day incubation period, the medium was carefully removed and the wells were filled with 100 μl of 3-[4,5 dimethyl-thiazol – 2 lyl]-2,5 diphenyl tetrazolium bromide (MTT) (Sigma, Münich, Germany) (1 mg/mL)

dissolved in a complete RPMI medium. Wells with 100 µl of MTT solution served as blank controls. After a 3-hour incubation period (37°C, 5% CO_2), 100 µl / well of 10% sodium – dodecyl sulphate (SDS) – 0.1N HCl (Serva, Heidelberg, Germany) was added to solubilize intracellularly stored Formosan. Plates were incubated overnight at room temperature. Optical density of the colour was then measured at 570 nm in a spectrophotometer (Behring ELISA Processor II, Ingelberg, Germany).

Results are expressed as the percentage of optical density (metabolic activity) compared to control (control conditioning medium), used as 100%.

2.5 Proliferation assay

The thymuses of Albino Oxford (AO) rats, male, 9 weeks old, bred at the Institute of Medical Research, MMA, Belgrade, Serbia were removed aseptically under general ether anaesthesia. The use of animals for the experiments was in accordance with the Guideline for the Use of Experimental Animals, approved by the Ethical Committee of the Military Medical Academy, Belgrade, Serbia (282-12/2002), which strictly follows the rules of the European Community Guidelines (EEC Directive of 1986; 86/609/EEC). Single cell suspensions of thymocytes were prepared by teasing the thymuses in an RPMI medium through a steel-mesh. After washing, the thymocytes were cultivated in the complete RPMI medium in 96-well flat bottom plates (ICN) ($1x10^6$ cells/well; 200 µl) for 72 hours in an incubator (Flow) with 5% CO_2 at 37°C. Cells were stimulated with 2.5 µg/ml of Concanavalin A (Con A) (Sigma). Different dilutions of Au-Pt conditioning media and the control conditioning medium or different concentrations of $ZnCl_2$ were added to the thymocytes. The cells were cultivated for 3 days. During the last 18 hours of cultivation the cells were pulsed with 1 µCi/well [^{3}H] thymidine (6.7 Ci/mmol, Amersham, Bucks, and U.K.). After harvesting, the radioactivity was counted using a scintillation counter (Beckman). The results were expressed as mean counts per minute (cpm) of triplicates. Proliferation activity was presented in percentages calculated on the basis of the proliferation activity of cultures with the control conditioning medium.

2.6 Apoptosis assays

Four methods were used for apoptosis. Unstimulated thymocytes, or ConA – stimulated thymocytes ($1x10^6$ cells / well / 200 µl complete RPMI medium), were cultivated in 96-well flat-bottom plates for 24 hours in the presence of Au-Pt conditioning media, a control medium, or different concentrations of $ZnCl_2$. For morphological evaluation, 10 µl of cell suspension was mixed with 30 µl of Türck reagent used for leukocyte counting, and apoptosis was evaluated by light microscopy (12). At least 500 cells of each triplicate were calculated. The results are given as percentages of apoptotic cells. The second method included the staining of cells with Annexin-FITC / Propidium iodide (PI) kit KNX50 (R & R, Abingdon, Oxon, UK). Cells from each well ($2x10^5$) were stained according to the manufacturer's instructions and analyzed using a flow cytometer (Coulter XL-MCL, Krefeld, Germany). Double-negative cells are viable cells, Annexin-FITC$^+$ / PI$^-$ cells represent thymocytes in the early stages of apoptosis, double positive cells are thymocytes in the late stages of apoptosis / secondary necrosis, whereas only PI$^+$ cells are primarily necrotic cells (13).

The third method was based on detecting a decrease in mitochondrial potential ($\Delta\varphi_m$), evaluated by the staining of cells with 3.3'-dihexyloxacarbocyanine iodide ($DiOC_6$) (Calbiochem, Ottawa, Canada) (14). Briefly, thymocytes from cultures ($2x10^5$) were incubated in phosphate buffered saline (PBS) containing 40 nM $DiOC_6$ for 15 mins at 37°C. The cells were washed, resuspended in PBS, and left at 37°C for 30 mins. Analysis was performed using a Coulter XL-MCL flow cytometer (fluorescence detection at 670 nm).

The fourth method included the detection of DNA fragmentation as revealed by the quantification of hypodiploid nuclei (15). For this purpose, thymocytes ($2x10^5$) were washed with PBS and incubated with 500 µl of PI (10 µg/ml) dissolved in a hypotonic solution (0.1% sodium citratis + 0.1% Triton-X solution in distilled water). Cells were incubated with PI for 4 hours at room temperature and then analyzed by flow cytometry.

2.7 Detection of IL-2 in culture supernatants

Con A – stimulated thymocytes were cultivated in 96-well flat bottom plates as described for proliferation assay. After 24 hours, cell-free supernatants were collected and stored at –20°C until assayed. For detection of IL-2 in these supernatants an ELISA detection system for rat IL-2 (R&D) was used as described by the manufacturer.

2.8 Detection of IL-2Rα expression

Thymocytes were cultivated with Au-Pt conditioning media or a control medium in the presence of ConA, for 2 days. After that, the cells were collected, washed with PBS containing 2% FCS and 0.1% sodium aside (PBS/FCS). Dead cells were removed using Nycoprep Animal gradient (density 1,077 g / cm^3) (Nycomed, Oslo, Norway). Viable cells from the interface zone were washed, adjusted at concentrations of 2 x 10^5 cells / tube and incubated at 4°C with anti-CD25 (OX-39) conjugated with FITC (Serotec, Oxford, UK) mAb (1 µg/ml) for 45 mins. The control cells were incubated with an irrelevant mAb - FITC. Labelled cells were fixed in 4% formalin and analyzed on an EPICS-XL-MCL flow cytometer as previously described (12).

2.9 Scanning electron microscopy (SEM)

Microstructural characterisation of the alloy samples was carried out by scanning electron microscopy (SEM-Sirion 400 NC), in addition to energy-dispersive X-ray (EDX) analysis (Oxford INCA 350). The specimens were only polished to minimize the influence of metallographic preparation regarding changes in chemical composition on the alloy

surface. After conditioning the samples were observed directly without any surface preparation. Concentrations of alloying elements in the analyzed phase were performed by at least 10 EDX measurements at different positions on the surfaces of grains.

2.10 X-ray diffraction (XRD) analysis

XRD analysis was used to determine the phase compositions of the alloys. The diffraction patterns were collected on a PANalytical X'pert PRO MPD diffractometer using reflection geometry and $CuK_{\alpha 1}$ radiation. The 2-theta range was from 30° to 120°. Measured diffraction patterns were compared using the X'Pert HighScore (PANalytical) computer programme. The Crystallographica Search Match (Oxford Cryosystems) programme was applied for qualitative phase analysis and crystallographic data of the identified phases were retrieved from the ICSD database (16). Quantitative phase analysis was performed by the Topas (Bruker AXS) programme, which uses the Rietveld method (17).

2.11 Statistics

The data are presented as a mean ± SD. The Student's *t*-test and one-way ANOVA test were used for statistical analysis of the results.

3 Results

3.1 Effect of Au-Pt – conditioning media on the metabolic activity of L929 cells

The first aim of this biocompatibility study was to test the effect of the extract from Au-Pt I and Au-Pt II alloys on the metabolic activity of L929 cells. As shown in Table 1, the Au-Pt I conditioning medium did not exert any statistically significant effect on the viability of L929 cells, whereas the Au-Pt II medium extract decreased the metabolic activity of the cells to 61.3 ± 5.0% ($p < 0.005$) compared to control.

The results of L929 cytotoxicity were compared with the concentrations of metals released from the alloys into the

Table 1

Comparison of the effect of Au-Pt conditioning media on the metabolic activity of L929 cells with the concentrations of released Zn ions

Conditioning medium	% metabolic activity of L929 cells[a]	Zn (µg/ml)
Control	100 ± 5.3	0.2
Au-Pt I	91.6 ± 4.2	1.6
Au-Pt II	61.3 ± 5.0***	5.3

[a] Values are given as mean ± SD (n = 6), calculated according to the optical density of cell cultures with control conditioning medium used as 100% (see Materials and methods)

*** = $p < 0.005$ compared to control or Au-Pt I medium (one-way ANOVA)

Figure 1

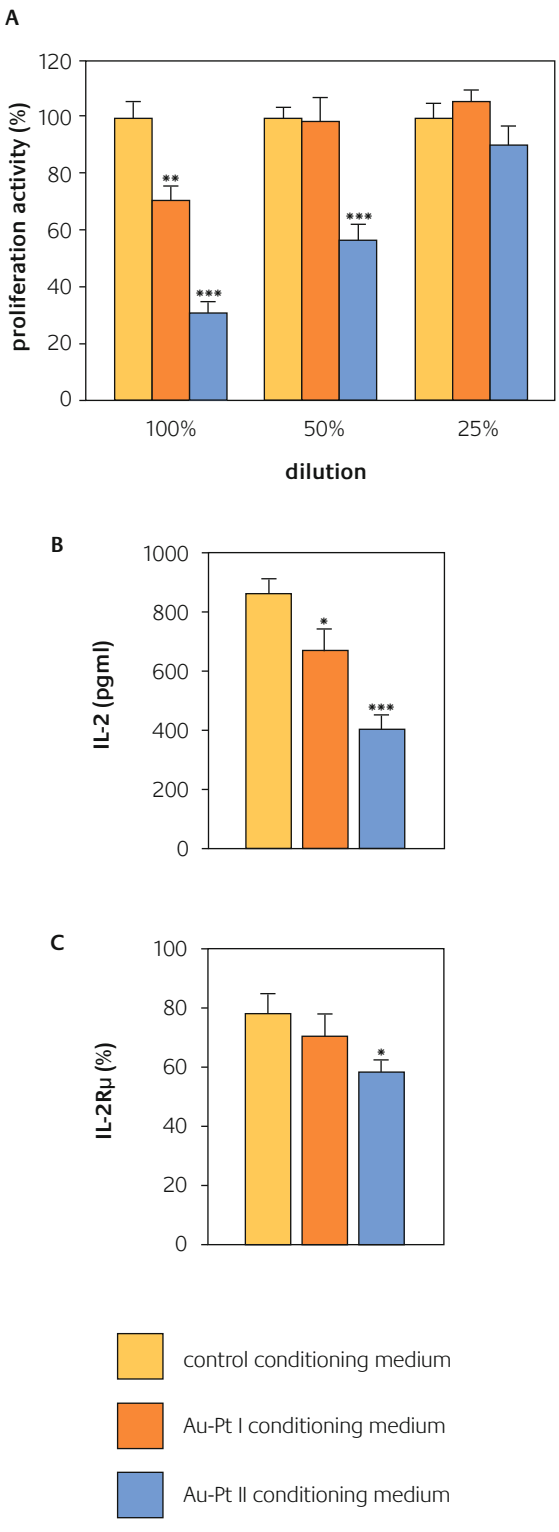

The effect of Au-Pt conditioning media on proliferation (A), production of IL-2 (B) and expression of IL-2Rα (C) by ConA-stimulated rat thymocytes. Thymocytes were cultivated with different dilutions of Au-Pt alloy's extracts as described in detail in Material and methods. The levels of IL-2 and the expression of IL-2Rα in cultures treated with undiluted conditioning media. Values are given as mean ± SD (n = 6) of one representative experiment.
** = $p < 0.05$; ** = $p < 0.01$; *** = $p < 0.005$ compared to corresponding control (Student`s t-test)*

culture medium (Table 1). The concentration of Zn was about 3 times higher in the Au-Pt II medium (5.3 µg/ml) than in the Au-Pt I medium (1.6 µg/ml). The concentration of Zn in the culture medium was 0.2 µg/ml. No other elements, including Au and Pt, were detected (detection limit: < 0.05 µg/ml).

3.2 The effect of Au-Pt conditioning media on rat T- cell proliferation

Our previous results showed that a T-cell proliferation assay is a more sensitive method for screening the cytotoxic acitivities of dental alloys than the conventional MTT assay on L929 cells (*Ristić et.al., manuscript submitted*). Therefore, we tested the effect of Au-Pt alloy extracts on the proliferation of rat thymocytes in the presence of ConA. The results, presented in Fig. 1A, demonstrate that an undiluted Au-Pt I medium concentration statistically significantly suppressed T-cell proliferation ($p < 0.05$) and the inhibition was about 30% compared to the control conditioning medium. The inhibition of T-cell proliferation in the presence of the Au-Pt II medium was higher and dose dependent. Undiluted medium reduced cellular proliferation by about 70%.

3.3 Mechanisms of the immunosuppressive activity of Au-Pt extracts

To explore those mechanisms involved in the suppression of T-cell proliferation we studied the production of IL-2, a dominant T-cell growth factor, and the expression of IL-2Rα by ConA – stimulated thymocytes. As seen in Fig. 1B, both Au-Pt media inhibited the production of IL-2, but only the Au-Pt II medium additionally down-regulated the expression of IL-2Rα.

The lower production of IL-2 and cellular proliferation caused by the Au-Pt alloy extracts might be a consequence of thymocyte apoptosis. To check this hypothesis, we examined the apoptosis of thymocytes using different methods. The results given in Table 2 show that neither Au-Pt medium modulates apoptosis of unstimulated thymocytes in the culture. However, the Au-Pt II medium potentiated ConA – induced apoptosis of thymocytes (Table 2, Fig. 2). The effect was observed during the early phase of apoptosis (nuclear condensation as revealed by Türk staining, and an increase in the percentage of Annexin V – $FITC^+/PI^-$ cells), as well as the reduction of

Table 2

The effect of Au-Pt alloy conditioning media on rat thymocyte apoptosis in cultures

Unstimulated cultures (% apoptosis/necrosis)

Medium	Morphol.	Anexin FITC / PI staining				PI staining	DiOC6 staining
		Total apoptosis/ necrosis	An-F^+/PI^-	An-F^+/PI^+	An-F^-/PI^+		
Control fresh	39.1 ± 3.7	41.4 ± 2.0	12.3±2.1	29.1±1.9	4.8±0.5	33.0±5.2	45.1±2.4
Control condition	41.2±3.3	44.0±2.1	11.4±1.6	33.2±2.1	5.0±0.6	36.1±4.1	47.2±1.8
Au-Pt I	42.6±3.0	39.9±2.1	10.2±2.2	28.6±1.7	5.1±0.4	32.6±2.7	44.2±2.3
Au-Pt II	44.4±2.5	42.1±2.1	10.8±0.7	31.0±2.5	5.9±0.4	34.6±1.8	44.8±1.9

ConA - stimulated cultures (% apoptosis/necrosis)

Medium	Morphol.	Anexin FITC / PI staining				PI staining	DiOC6 staining
		Total apoptosis/ necrosis	An-F^+/PI^-	An-F^+/PI^+	An-F^-/PI^+		
Control fresh	50.1±1.9	53.0±1.8	6.1±0.8	46.9±2.4	5.6±0.5	46.7±1.6	64.1±2.9
Contol condition	52.2±3.1	58.2±2.4	5.5±0.8	52.8±1.9	6.5±0.6	48.4±1.3	74.8±2.7
Au-Pt I	48.8±2.6	62.1±2.0	8.1±1.1	54.7±2.5	6.9±1.4	47.6±2.9	78.2±4.2
Au-Pt II	61.3±3.1*	64.1±2.6	11.4±2.5**	52.0±2.6	6.1±0.4	50.1±2.6	83.7±2.8*

Unstimulated, or ConA-stimulated thymocytes ($1x10^6$ / well), were cultivated for 24hours with a fresh medium or undiluted conditioning media, following which apoptosis was determined using four different methods as described in Material and methods.

Results of one representative experiment are given as mean ± SD (n = 6)

* = $p < 0.05$; ** = $p < 0.01$ compared to control conditioning medium (one-way ANOVA)

Figure 2

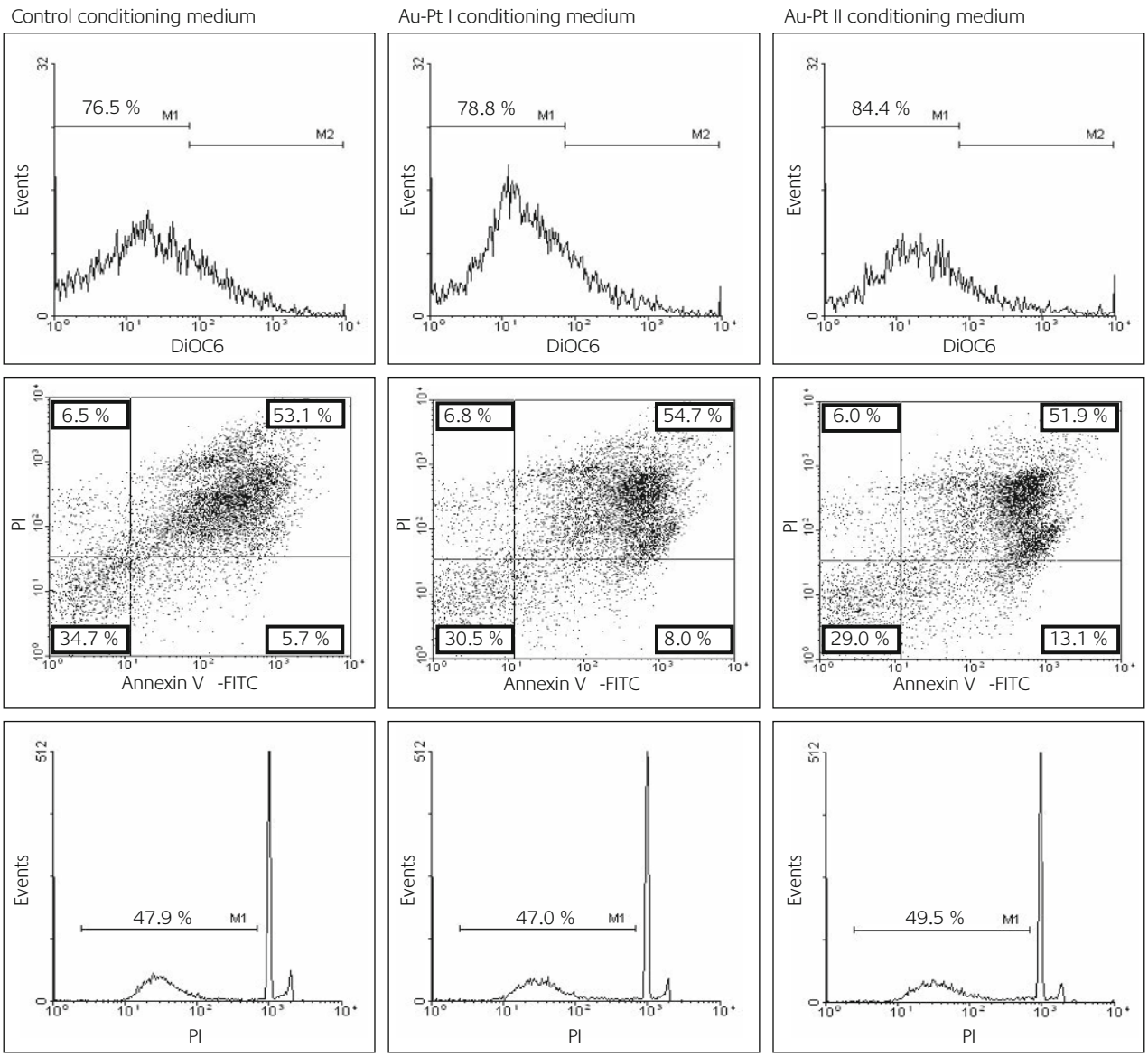

The effect of Au-Pt conditioning media on apoptosis of ConA-stimulated thymocytes.
Representative histograms: staining with $DiOC_6$ (first row); double staining with PI and Annexin V FITC (middle row); PI staining of thymocytes treated with hypotonic buffer (third row). The cut-off on $DiOC_6$ fluorescence profiles was set up on the basis of the fluorescence of viable, freshly isolated thymocytes.

mitochondrial membrane potential ($DiOC_6$ staining), but not at the level of DNA fragmentation (PI staining of hypodiploid nuclei).

3.4 The effect of Zn ions on the cytotoxicity of L929 cells and the functional characteristics of rat thymocytes

We compared the effect of exogenously added Zn ions on L929 cells and thymocytes, because Zn was the only detectable element released from Au-Pt alloys in this study and, in addition, this element is an important modulator of apoptosis (18). Zn was used in 4 different concentrations (1.6 µg/ml, 5.3 µg/ml, 7.5 µg/ml and 10.0 µg/ml), of which the first two were equal to Zn concentrations found in the Au-Pt I and Au-Pt II media respectively. The results (Table 3) show that Zn, the dose-dependent, inhibited the metabolic activity of L929 cells, the proliferation of thymocytes and the production of IL-2, but did not significantly alter the apoptosis of the unstimulated thymocytes. The potentiation of ConA-induced apoptosis of thymocytes was seen only with the highest concentration of Zn. In addition, the concentrations of Zn comparable to those detected in the Au-Pt alloy conditioning media did not exert any significant adverse effect on the L929 cells and showed a lower immunosuppressive effect on the thymocytes, compared to alloy extracts.

Table 3

The effect of different concentrations of $ZnCl_2$ on the metabolic activity of L929 cells, the proliferation of ConA - stimulated thymocytes and production of IL-2 (A) and apoptosis of thymocytes (B).

A) L929 cells (metabolic activity); Thymocytes (proliferation and IL-2 production)

Zn^{2+} (µg/ml)	MTT (L929) (% to control)	Proliferation (% to control)	IL-2[a] (pg/ml)
Control	100.0 ± 4.8	100.0 ± 7.2	766.2 ± 31.6
Zn^{2+} (1.6 µg/ml)	102.6 ± 3.9	95.2 ± 11.1	758.1 ± 66.7
Zn^{2+} (5.3 µg/ml)	91.2 ± 6.6	51.3 ± 4.7***	608.2 ± 35.4*
Zn^{2+} (7.5 µg/ml)	38.4 ± 2.7***	18.1 ± 3.0***	180.2 ± 13.4***
Zn^{2+} (10.0 µg/ml)	0.6 ± 0.1***	0.1 ± 0.1***	12.1 ± 1.9***

B) Apoptosis of thymocytes

	Unstimulated cultures		ConA – stimulated cultures	
Zn^{2+} (µg/ml)	Morphology (%)	$DiOC_6$ staining (%)	Morphology (%)	$DiOC_6$ staining (%)
Control	38.1 ± 3.6	44.1 ± 3.7	49.1 ± 3.0	52.1 ± 1.6
Zn^{2+} (1.6 µg/ml)	35.1 ± 4.8	45.1 ± 7.3	46.1 ± 2.9	50.2 ± 1.3
Zn^{2+} (5.3 µg/ml)	36.2 ± 3.9	42.6 ± 3.3	45.1 ± 3.7	55.6 ± 3.4
Zn^{2+} (7.5 µg/ml)	33.6 ± 4.0	40.1 ± 6.1	54.0 ± 1.8	60.1 ± 3.3*
Zn^{2+} (10.0 µg/ml)	33.9 ± 4.9	44.8 ± 5.0	57.1 ± 3.0*	67.2 ± 3.0**

A detailed description of the methodology is given in Material and methods. Values are given as mean ± SD (triplicates) of one representative experiment.

* = $p < 0.05$; ** = $p < 0.01$; *** = $p < 0.005$ compared to control ([a]Student's t-test and one-way ANOVA)

3.5 Microstructural analysis of Au-Pt alloys before and after conditioning in the culture medium

The microstructural analysis of Au-Pt alloys was performed by SEM, EDX and XRD. The results are presented in Table 4, Fig 3. and Fig 4. The Au-Pt I alloy was composed of an Au – dominant α_1 phase (98.44 wt. %) and a minor, Pt – dominant α_2 phase (1.56 wt. %). On the other hand, the Au-Pt II alloy additionally contained three minor phases ($AuZn_3$, Pt_3Zn and $Au_{1.4}Zn_{0.52}$) and the calculated mass ratio (wt. %) was: α_1: α_2: $AuZn_3$: Pt_3Zn: $Au_{1.4}Zn_{0.52}$ = 95.55: 2.72: 0.98: 0.24: 0.5. The phases in these alloys were identified and analysed according to the lattice parameters, their comparison with pure Au and Pt and binary $AuZn_3$, Pt_3Zn and $Au_{1.4}Zn_{0.52}$ phase diagrams (*Rudolf et al., manuscript in preparation*). The α_1 phase of Au-Pt I was richer in Pt and poorer in Au compared to the α_1 phase of Au-Pt II. The opposite results were obtained for the α_2 phase. The content of Zn in both α_1 and α_2 phases of the Au-Pt II alloy was higher compared to the Au-Pt I sample. The other three minor phases were enriched with Zn and the highest content was detected in the Pt_3Zn phase, followed by $Au_{1.4}Zn_{0.52}$ and $AuZn_3$.

After conditioning the surface of specimens were examined directly without any metallographic preparation, with the aim of discovering the interaction of sample surfaces with conditioning media during *in vitro* experiments. The EDX-point analysis for all detected phases showed that the α_1-phase regions became poor in Zn and within them there was no Rh, In and Ir (Table 4). The α_2 phases also contained smaller portions of Zn and Rh and consequently higher concentrations of Au and Pt. Diffraction patterns for the Au-Pt I alloy (Fig 4.) showed the presence of another group of peaks (marked $\alpha_{2\text{-}s}$), shifted from the α_2 phase by approximately 1°, most probably as a consequence of micro-segregation in the middle of the α_2 phase. The calculated mass ratio (wt. %) for the phases of Au-Pt I after conditioning was: α_1:α_2:$\alpha_{2\text{-}s}$ = 90.82: 4.50: 4.67.

Contrary to this, the number of detected phases in the Au-Pt II alloy was lowered from 5 to 3 after biocompatibility conditioning. The $AuZn_3$ and Pt_3Zn phases disappeared from the surface of Au-Pt II alloy such that the calculated mass ratio for the existing phases was α_1:α_2: $Au_{1.4}Zn_{0.52}$ = 94.28: 4.67: 1.05.

Table 4

Average results of EDX phase analyses in the Au-Pt alloys before (A) and after (B) conditioning (in wt. %)

		Au	Pt	Zn	Rh	In	Ir
Au –Pt I							
α_1 phase	A	90.18 ± 1.68	7.45 ± 1.55	1.16 ± 0.24	0.36 ± 0.31	0.19 ± 0.15	0.66 ± 0.38
α_1 phase	B	97.31 ± 3.34	2.03 ± 2.58	0.66 ± 0.21	/	/	/
α_2 phase	A	21.63 ± 8.22	73.62 ± 4.33	0.36 ± 0.26	3.86 ± 0.77	0.53 ± 0.37	/
α_2 phase	B	22.07 ± 3.74	74.91 ± 3.51	0.27 ± 0.18	2.75 ± 0.72	/	/
Au –Pt II							
α_1 phase	A	97.36 ± 0.43	0.16 ± 0.10	1.34 ± 0.26	0.25 ± 0.17	0.21 ± 0.15	0.68 ± 0.48
α_1 phase	B	98.91 ± 0.24	0.21 ± 0.14	0.88 ± 0.22	/	/	/
α_2 phase	A	15.82 ± 10.49	79.39 ± 17.64	0.96 ± 0.49	3.60 ± 1.40	0.23 ± 0.18	/
α_2 phase	B	16.06 ± 0.92	80.39 ± 2.13	0.29 ± 0.18	3.13 ± 0.04	0.13 ± 0.06	/
Pt_3Zn phase	A	2.34 ± 0.37	91.66 ± 3.38	3.96 ± 1.41	1.58 ± 0.38	0.46 ± 0.13	/
Pt_3Zn phase	B	/	/	/	/	/	/
$AuZn_3$ phase	A	98.05 ± 0.25	/	1.95 ± 0.25	/	/	/
$AuZn_3$ phase	B	/	/	/	/	/	/
$Au_{1.4}Zn_{0.52}$ phase	A	88.85 ± 2.13	7.67 ± 1.55	3.17 ± 0.60	0.31 ± 0.04	/	/
$Au_{1.4}Zn_{0.52}$ phase	B	92.92 ± 2.55	5.67 ± 1.58	1.04 ± 0.45	0.37 ± 0.21	/	/

Values are given as mean ± SD (wt. %) for 10 measurements

4 Discussion

In this work we have compared the microstructure of two experimental high noble Au-Pt dental alloys with their biocompatibility *in vitro*. Such types of Au-Pt alloys may be used for full cast or metal ceramic applications (18). Although the unit cost of these two metals is high, the alloys have advantages in the clinical use, especially for single – tooth restoration, over lower cost high – Pd alloys of similar biomechanical characteristics, due to higher biocompatibilities and non-allergenic properties (6,7,19). The successful clinical application of a high noble alloy for metal ceramic bonding depends on many factors, including metal ceramic compatibility (20). However, *in vitro* tests of biocompatibility are a primary demand for any alloy potentially to be used in contact with living tissues. Therefore, biocompatibility testing was the principal goal of this study. We decided to test the effect of Au-Pt conditioning media because this approach enables simultaneous quantification of released metal ions.

The first biocompatibility assay was based on the determination of mitochondrial SDH activity in a mouse fibroblast cell line (L929). This screening cell viability test, recommended by ISO (1997), has commonly been used for the evaluation of the biocompatibility of dental materials. We showed that the medium of Au-Pt I alloy did not exert any statistically significant effect on the viability of L929 cells, but surprisingly, the Au-Pt II medium reduced cell viability by about 40%. These results clearly correlated with the concentrations of Zn ions which were about three times higher in the Au-Pt II extract (5.3 µg/mL *versus* 1.6 µg/mL).

Figure 3

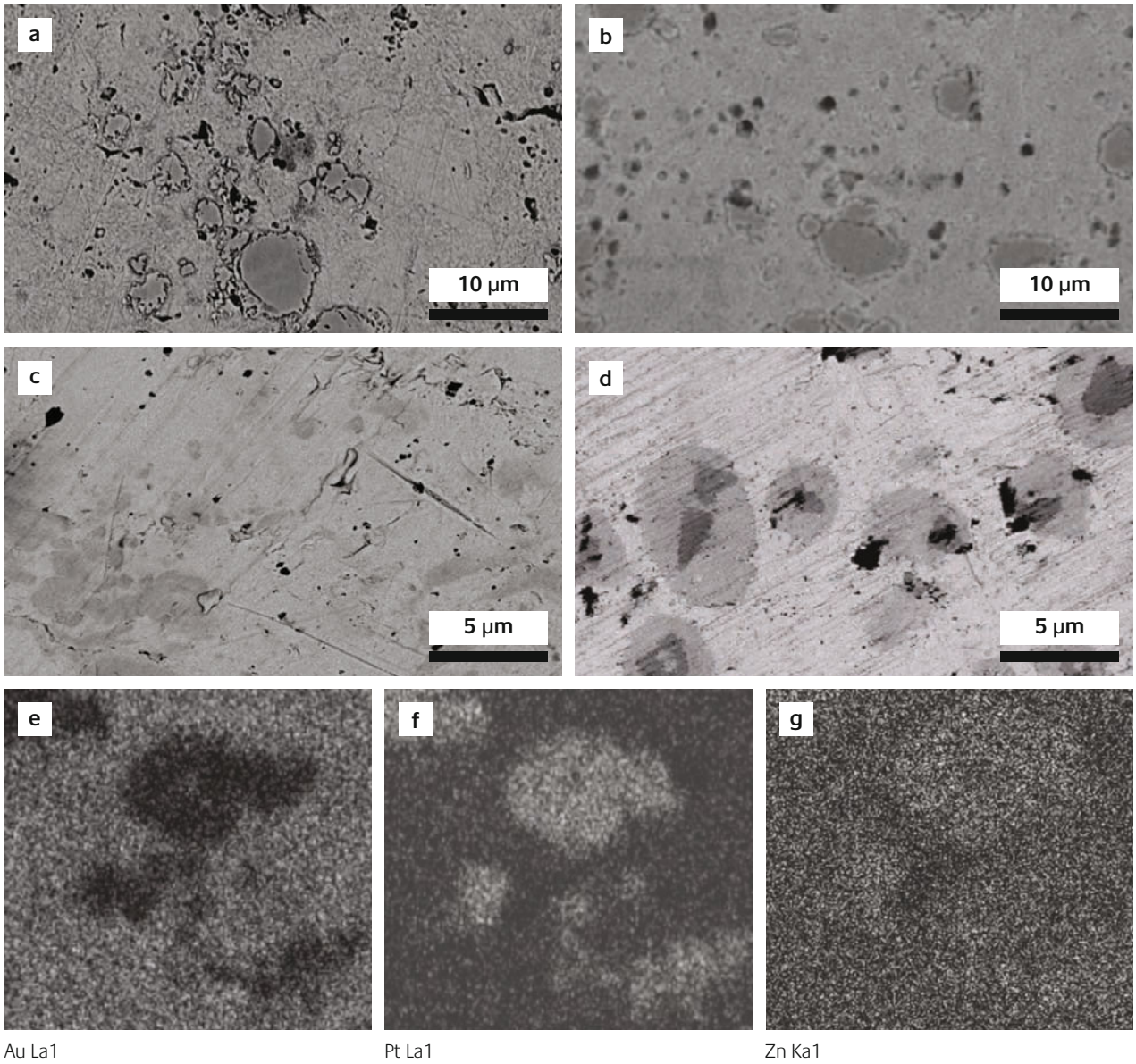

The SEM microstructure of Au-Pt alloys before and after conditioning and EDX chemical mapping of the elements in the region of the Au-Zn and Pt-Zn phases in the Au-Pt II alloy.
a) SEM of Au-Pt I before conditioning; b) SEM of Au-Pt II before conditioning;
c) SEM of Au-Pt I after conditioning; d) SEM of Au-Pt II after conditioning;
e) EDX mapping of Au; f) EDX mapping of Pt; g) EDX mapping of Zn.

No other elements, including Au and Pt, were detected, which is in accordance with the results of other researchers on the alloys of similar composition (7-9).

When evaluating the cytotoxicity of metal ions it is important that their concentrations in conditioning fluids reach the levels to cause a detectable adverse effect. The concentrations of released metal ions depends on the corrosion properties of an alloy in an immersion solution, but also on the ratio of surface area of a specimen to a volume of solution and the duration of conditioning. Most authors investigating the corrosion of dental alloys follow the recommendations by ISO (1997), (surface area-to volume ratio: 0.5-6.0 cm^2/mL; period of conditioning: 3-7 days; immersion solutions: distilled water, acidified artificial saliva or culture media). As can be seen, the range of these parameters is rather broad, and because of that it is difficult to make exact comparisons of the results obtained in different laboratories.

Al-Hyasat *et al.*,(8) showed that the release of Zn (167±6.5 ppb) from Bioherador N, a high noble Au-Pt alloy, composed of 86.2 wt. %Au, 11.2 wt. %Pt and 1.5 wt. %Zn in distilled water (0.5 cm^2/mL) after 7 days was still insufficient to cause a significant biological effect. However, the tested concentration was only 10% of the aqueous alloy extract

Figure 4

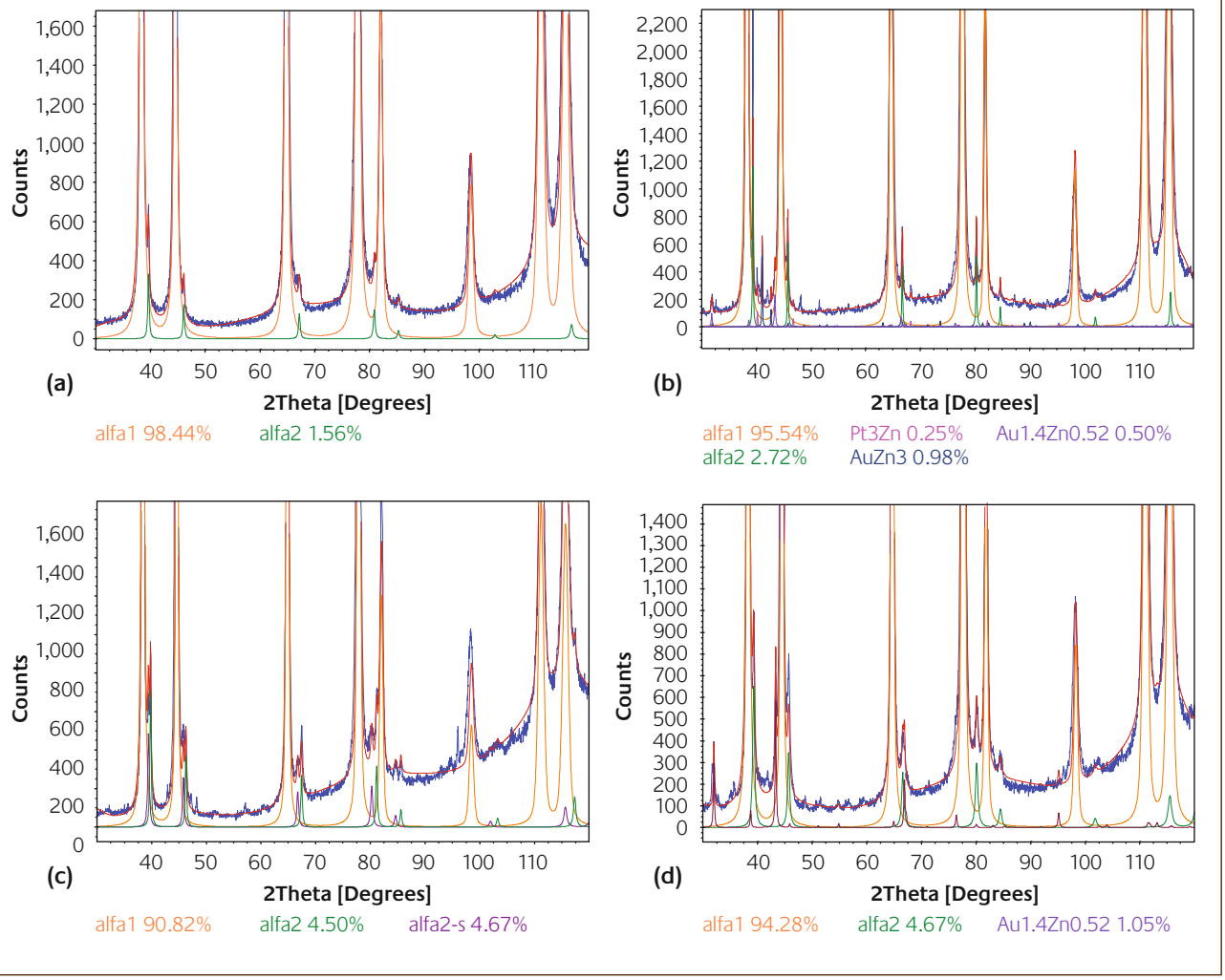

Rietveld plots for the Au-Pt alloys before and after conditioning.
a) Au-Pt I before conditioning; b) Au-Pt II before conditioning;
c) Au-Pt I after conditioning; d) Au-Pt II after conditioning.

diluted in DMEM medium with 5% FCS. We used a different approach for preparation of the Au-Pt extracts, including exposing a higher surface area to fluids (1.88 cm^2/mL), longer conditioning (three rounds of two-week periods) and a different culture medium (RPMI + 10% FCS). In comparison with our results, Schmaltz *et al.*, (9), found a lower concentration of Zn (about 0.5 µg/mL) in the alloy extract after a 7-day conditioning time of two high noble Au alloys (0.8 cm^2/mL of Eagle basal culture medium with 5% FCS). Moreover, the basic composition of these alloys significantly differed from our Au-Pt alloys and, except for Au, Pt, and Zn, the alloys contained Ag, Cu and Pd. Similarly, Celebic *et al.*, (21) studied the release of Zn from a commercial Au-Pt dental alloy composed of 75.0 wt. % Au, 8.0 wt.% Pt, 9.5 wt.% Ag, 5.1 wt.% Cu and a trace amount of Zn (1.5 wt.% together with Cu in the brass), using different immersion solutions (artificial saliva, acidic phosphate buffer or organic acid mixture), (1.14 cm^2/mL), over different periods of time up to 30 days. Although the levels of Zn slightly varied depending on the immersion solution, the detected concentrations of this element were in the range of about 0.1-0.25 µg/mL, independently of cultivation time, below the Zn concentrations that we measured in both Au-Pt solutions. Wataha *et al.*, (7), showed that a high noble Au-Pt alloy composed of 83.4 wt.% Au, 11.4 wt.% Pt and relatively high Zn content (4.4 wt.%), released a similar concentration of Zn ions in a DMEM medium with 3% Nu serum (1.26 cm^2/mL), after 7 days, as we measured in the Au-Pt II medium. The concentration of released Zn increased up to 10 times in saline-BSA solution. Although the cytotoxicity of this medium was not studied, previous results from the same group (22) with an Au-Pt alloy composed of 85wt.% Au, 11.7 wt.% Pt and 1.5 wt.% Zn, showed a reduction of the metabolic activity of Balb/c 3T3 fibroblasts (direct immersion assay; 3 days) of about 20-25%.

More than 85% of thymocytes are immature T cells with a

short lifespan, both *in vivo and in vitro*. The rest of them are more mature cells which proliferate very strongly *in vitro* in the presence of endogenous antigen-presenting cells (APC) and T-cell mitogens, such as ConA. Due to these characteristics (sensitivity to the proapoptotic/toxic and proliferation-modulating stimuli, rodent thymocytes have been used extensively in immunological and toxicological studies.

Based on our previous results (*Ristic et al., manuscript submitted*), which showed that the proliferation of rat thymic and spleen lymphocytes is a more sensitive parameter for evaluation of the biocompatibility of different high noble and base dental alloys than the standard MTT assay on L929 cells, in this work we wanted to check this hypothesis using Au-Pt alloys, having in mind also some contradictory literature data regarding the sensitivity of thymocytes to Zn ions (20,23,24). We showed that the Au-Pt I conditioning medium, although non-toxic for L929 cells, reduced the proliferative response of thymocytes by about 30%. Similarly, the Au-Pt II medium showed a stronger inhibitory effect on thymocytes (reduction of proliferation by about 70%), compared to the metabolic activity of L929 cells (Table 1) or the proliferation of L929 cells with or without ConA (data not shown).

It is well known that ConA, a polymeric plant lectin, is a very potent mitogen for T cells. After cross-linking of TCR and accessory molecules, including mannose-containing receptors, on T cells and APC, ConA triggers activation and proliferation of T cells. The process is followed by the expression of IL-2Rα and production of IL-2. As mentioned above, it is believed that in the ConA-stimulated culture of thymocytes, proliferation is restricted to mature T cells with high expression of the T cell receptor (TCR) (25). We found that the Au-Pt I medium inhibited the production of IL-2, non affecting IL-2Rα expression and apoptosis. However, the Au-Pt II medium suppressed thymocyte proliferation by decreasing both the production of IL-2 and the expression of IL-2Rα. In addition, this medium potentiated the ConA-induced apoptosis of thymocytes (26). Based on these findings it can be hypothesized that reduction in the cell number, due to apoptosis, could be an additional factor responsible for the suppression of IL-2 production, decreased number of IL-2Rα$^+$ cells and more profound inhibition of thymocyte proliferative activity in cultures with the Au-Pt II extract.

An important question resulting from this work is whether Zn ions are responsible for the observed cytotoxicity of the Au-Pt conditioning media. It is well-known that Zn is one of the most important trace elements in the body and it is essential as a catalytic, structural and regulatory ion. It is involved in homeostasis, immune responses and ageing (27). A significant cytoprotective activity of Zn is related to its integration with proteins, maintaining cellular stability. However, changes in Zn status and its intracellular concentrations have been associated with several pathological states. The intracellular Zn overload may disturb cell redox balance, leading to oxidative stress and apoptosis (28,29).

Contrary to the previous results, several reports showed that Zn inhibits the apoptosis of thymocytes (20,23,30). The effect may be caused by the inhibition of reactive oxygen species production (31), suppression of caspase-3 (23), or the stabilization of damaged cell membranes by competing with intracellular Ca (32). In our study we did not detect any significant effect of Au-Pt media or Zn ions on thymocyte apoptosis, contrary to the results of Chukhlovin *et al*., (20) who found that Zn (100 μM) suppressed the apoptosis of rat thymocytes after a 3-hour incubation period. The difference between our and their results could be explained by the fact that we studied apoptosis after a longer incubation time (24 hours).

However, our results on ConA-activated thymocytes showed that both Au-Pt II medium and higher doses of Zn ions stimulated apoptosis. The effect was manifested as the reduction of mitochondrial membrane potential and the expression of phosphatidyl-serine on the outer cell membrane, as revealed by increased binding of Annexin V (14). Although we detected an increase in the percentage of cells with condensed nuclei, the fragmentation of DNA, as a final step in the apoptotic process, was not observed. These findings are in accordance with the previous results on malignant cells, endothelial cells and neuronal tissue, which demonstrated that Zn can, directly or indirectly, stimulate mitochondrial alterations leading to apoptosis (28,29). It seems that ConA-activated thymocytes respond differently to Zn stimuli than resting thymocytes, because the apoptotic pathways in non-activated and activated T cells differ considerably (33). This hypothesis could be supported by the findings that Zn ions stimulate the phosphoionositide 3-kinase/Akt signalling in several cell types. However, the cellular outcome of Akt activation with respect to apoptosis differs significantly with cell type (*i.e.* stimulation of apoptosis in neuronal cells; inhibition of apoptosis in airway epithelial cells) (34).

Based on SEM, EDX and XRD analyses of both Au-Pt alloys' microstructures before biocompatibility testing, we concluded that Au-Pt I consists of two phases, while in the Au-Pt II alloys there are at least five phases (*Rudolf et al., manuscript submitted*). In both microstructures the main phase is cubic fcc α_1 with a crystal structure of pure gold, while the minor cubic fcc α_2 phases have very similar lattice parameters to Pt (35-37). According to the investigated microstructure and simultaneous thermal analysis (STA) (*Rudolf et al., manuscript submitted*) we assume that during manufacturing in the case of Au-Pt I melt the thermodynamic conditions were almost at equilibrium and, consequently, only two phases were formed during the solidification process. On the other hand, the manufacturing conditions for Au-Pt II melt were non-equilibrium because the final microstructure contained three additional minor phases: $AuZn_3$, Pt_3Zn and $Au_{1.4}Zn_{0.52}$. These phases were mostly segregated at the grain boundaries between α_1 and α_2 phases. Such manufacturing conditions caused conditions at solidus temperature which enabled the remaining Au-Pt II

melt to become locally-enriched with Zn leading to different phase precipitation, which finally results in improved mechanical properties for the Au-Pt II alloy compared to Au-Pt I (38,39).

The general conclusion of the EDX and XRD analyses after conditioning is that all phases were prone to corrosion, but the decrease of Zn content in both α_1 and α_2 phases of the Au-Pt II alloy was significantly lower compared to the Au-Pt I alloy. These results, together with the finding that the Pt_3Zn and $AuZn_3$ phases completely disappeared, are in accordance with the higher release of Zn from the Au-Pt II alloy in the culture medium.

Our results are in general agreement that multiphase alloys are less corrosion resistant than single phase alloys (40) due to their different electrode potential. When an alloy is immersed in an electrolyte such as a tooth environment or cell culture medium, any meta-stable phase is less resistant to corrosion than the homogenized solid solution because of the differences in electrode potential caused by microsegregation and variation in composition between individual dendrites. However, to our knowledge, our study is the first one which directly investigated the changes in microstructure of high noble Au-Pt alloys before and after conditioning and correlation of the corrosion processes at the microstructural level with the release of alloying elements.

One significant conclusion of this work is that Zn was not the only factor responsible for the observed biological effects of Au-Pt media, because our comparative study with the same concentrations of exogenous Zn^{2+} ions showed a lesser adverse effect of Zn than the conditioning media. There are at least two possibilities in explanation of this phenomenon. At first, some other metal ions, although undetectable in our cultures, might act synergistically with Zn. As shown by our EDX and XRD analyses of the single phase, the mass fraction of all other microalloying elements, including Ir, Rh and In, was lower or undetectable in the surface layer after conditioning. At the moment we do not know how these trace elements in the conditioning media interact with Zn with regard to the biocompatibility. Secondly, after prolonged cultivation for 2 weeks, Zn, and maybe other released elements, could modify some medium components, especially those present in serum, including Zn-binding proteins, and which in turn modulate the cellular response. Generally, our results contradict those published by other authors, (9) who showed that alloy extracts had lesser cytotoxic effects than the same concentrations of Zn salt. The difference could be explained by the different composition and microstructure of alloys, different mode of alloy conditioning, different cell culture media and different biological parameters that were monitored.

5 Conclusions

Several main conclusions can be drawn from this study. 1. The microstructure, but not the composition, of a high noble Au-Pt alloy is connected with its corrosion properties and biocompatibility *in vitro*. 2. The presence of $AuZn_3$ and Pt_3Zn phases in the alloy led to lower corrosion stability. 3. T-cell functional tests are more sensitive for evaluating the adverse effect of Au-Pt alloys than a conventional MTT assay on L929 cells. 4. The influence of whole Au-Pt alloy extracts on the biocompatibility is more complex than the effect of Zn alone, although Zn was the only detectable element released from the alloys. 5. The microstructural and XRD analyses of dental alloys before and after conditioning, in combination with the analysis of element release from the alloys, could be a new approach in explaining the results of biocompatibility assays.

Acknowledgements

This paper is part of a Slovenian Applied Project no. L2-7096, Bilateral Project SLO/SR BI-CS/06-07-031 and EUREKA Programme E!3555 DEN-MAT. The authors thank Zlatarna Celje d.d., Celje, Slovenia, working on the development of a new high Au content dental alloy, and associates from the Institute of Materials Technology, Faculty of Mechanical Engineering, University of Maribor; University of Ljubljana, Faculty of Natural Sciences and Engineering, School of Dentistry, University of Belgrade and Institute of Medical Research, Military Medical Academy, Belgrade, Serbia for their support and assistance.

The authors also gratefully acknowledge the Ministry of Higher Education, Science and Technology and Slovenian Research Agency.

About the authors

Miodrag Colic, MD, PhD is a full Professor of Immunology at the Military Medical Academy (MMA), Belgrade, Serbia and at the Medical School, University of Nis, Serbia. He is the Head of the Institute for Medical Research, MMA, and a member of the Serbian Academy of Sciences and Arts. His field of research is mainly focused on cellular immunology, inflammation, biotechnology, and the biocompatibility of dental and medical implants. To date he has published over 100 scientific papers in SCI journals.

Prof. Dr. Dragoslav Stamenkovic, Dean of the Faculty of Stomatology, University of Belgrade was born in 1949 in Belgrade. Having his Ph.D. since 1983, University of Belgrade he fills the positions of Dean and Professor at the Faculty of Stomatology. Study visits: Welsh National School of Medicine, University of London, University Medical Centre, Aachen, Trinity College and the Dental Hospital, Dublin. Main fields of research: Prosthodontics, Dental materials, Implantology.

Prof. Dr. Ivan Anzel was born in Slovenia in 1962. He obtained his Ph.D. in Physical Metallurgy at the University of Ljubljana, 1996. Positions: Professor in Materials Science, Head of the Institute of Materials Technology, Faculty of Mechanical Engineering, University of Maribor. Main fields of research: High Temperature and Internal Oxidation, Electron Microscopy and Analysis, Monitoring of Phase Transformations.

Assist. Prof. Dr. Gorazd Lojen was born in 1962 in Maribor, Slovenia. Since 1991 he has been a member of the Institute of Materials Technology, Faculty of Mechanical Engineering at University of Maribor. He obtained his Ph.D. in Mechanical Engineering in 2002, was habilitated to assistant professor in materials in 2005. His main fields of research: metal matrix composites, semisolid and shape memory alloys.

Dr. Rebeka Rudolf, Senior Researcher joined the Institute of Materials Technology in 1993. In 2002 she obtained her Ph.D. in mechanical engineering. Positions: Senior researcher at the Institute of Materials Technology, Development Manager and Head of the Research group in Zlatarna Celje. Fields of interest: Noble metals and alloys for jewellery and dentistry, new production technologies.

References

1 D. Williams (ed.), *Medical & Dental materials*, 1990, Oxford OX3, England

2 R.L. Bertolotti, in: W.J. O`Brien (ed.), *Dental materials: properties and selection* **323**, 1989, p. 240. Chicago: Quintessence

3 J. Fischer, *Dent. Mater.* 2002, **18**, 331

4 H. Knosp, R.J. Holliday, C.W. Corti, *Gold Bulletin*. 2003, **36**, 93

5 J.N. Wang, W.B. Liu, *Gold Bulletin*. 2006, **36**, 3

6 C.T. Hanks, J.C. Wataha, Z.L. Sun, *Dent. Mater.* 1996, **12**, 186

7 J.C. Wataha, S.K. Nelson, P.E. Lockwood, *Dent. Mater.* 2001, **17**, 4069

8 A.S. Al-Hiyasat, O.M, Bashabsheh, H. Darmani, *Int. J. Prosthodont.* 2002, **15**, 473

9 G. Schmalz, H. Langer, H. Schweikl, *J. Dent. Res.* 1998, **77**, 1772

10 R.G. Craig, C.T. Hanks, *J. Dent. Res.* 1990, **69**, 1539

11 R. Rudolf, T.H. Zupancič, L. Kosec, A. Todorovic, B. Kosec, I. Anžel, Metalurgija. (Sisak), 2008, **47**, 203

12 M. Colic, S. Gasic, D. Vucevic D, Lj. Pavicic, P. Popovic, D. Jandric, Lj. Medic-Mijacevic, Lj. Rakic, *Int. J. Immunopharmacol.* 2000, **22**, 203

13 I. Vermes, C. Haanen, H. Steffens-Nakken, C. Reutelingsperger, *J. Immunol. Methods.* 1995, **184**, 39

14 G. Macouillard-Poulletier, M.A. Belaud-Rotureau, P. Voisin, N. Leducq, F. Belloc, P. Canioni, P. Diolez, *Cytometry.* 1998, **33**, 333

15 K. Migita, K. Eguchi, Y. Kawabe, A. Mizokami, T. Tsukada, S. Nagataki, *J. Immunol.* 1994, **153**, 3457

16 ICSD database (latest update 2007-1, FIZ Karlsruhe. http://www.fiz-karlsruhe.de/icds.html

17 J.C. Taylor, *Rietveld: Practical guide*, 2001, Canberra

18 A.B. Chukhlovin, S.V. Tokalov, A.S. Yagunov, J. Westendorf, H. Reincke, L. Karbe, *Sci. Environm.* 2001, **281**, 153

19 J.C. Wataha, *J. Prosthet. Dent.* 2002, **87**, 351

20 M. Bagby, S.J. Marshall, G.W. Marshall, *J. Prosthet. Dent.* 1990, **63**, 21

21 A. Celebic, M. Baucic, J. Stipetic, I. Baucic, S. Miko, B. Momcilovic, *J. Mater. Sci. Mater. Med.* 2006, **17**, 301

22 J.C. Wataha, P.E. Lockwood, S.K. Nelson, S. Bouillaguet, *Int. J. Prosthodont.* 1999, **12**, 242

23 F. Chai, A.Q. Truong-Tran, L.H. Ho, P.D. Zalewski, *Immunol. Cell. Biol.* 1999 **77**, 272

24 W.G. Telford, P.J. Fraker, *J. Cell. Physiol.* 1995, **164**, 259

25 N.A. Nicola, *Stem Cells.* 1994, **1**, 3

26 F. Nagase, T. Abo, K. Hiramatsu, S. Suzuki, J. Du, I. Nakashima, *Microbiol. Immunol.* 1998, **42**, 567

27 M. Stefanidou, C. Maravelia, A. Dona, C. Spiliopoulou, *Arch. Toxicol*. 2006, **80**, 1

28 K.E. Dineley, T.V. Votyakova, I.J. Reynolds, *J. Neurochem*. 2003, **563**, 570

29 E. Rudolf, K, Rudolf, J. Radocha, J. Peychi, M. Cervinka, *Biometals*. 2003, **16**, 295

30 C. Yuan, M. Kadiiska, W.E. Ashansar, R.P. Mason, M.P. Waalkers, *Toxicol. Appl. Pharmacol*. 2000, **164**: 312

31 C.T. Walsh, H.H. Sandstead, A.S. Prasad, P.M. Newberne, P.J. Fraker, *Environ. Health. Persp*. 1994, **102**, 5

32 A.S. Prasad, *Ann. Intern. Med*. 1996, **125**, 142

33 C.R. Budd, *Curr. Opin. Immunol*. 2001, **13**, 356

34 A. Barthel, E.A. Ostrakhovitch, P.L. Walter, K. Kampkötter, L.O. Klotz, *Arch. Biochem. Biophys*. 2007, **463**, 175

35 S.P. Singhal, H. Herman, and J.K. Hirvonen, *Appl. Phys. Lett*., 1978, **32**, 25

36 Y. Khan, B.V.R. Murty, K. Schubert, *J. Less-Common: Met*., 1970, **21**, 293

37 K. Gotzman, U. Burkhardt, M. Ellner, *Grin Powder Diffraction*, 1997, **12**, 248

38 I. Anžel, A.C. Kneissl, L. Kosec, R. Rudolf, L. Gusel, *Z. Met.kd*., 2003, **94**, 9

39 C.W. Corti, *Gold Bull*., 1999, **32**, 2

40 K.J. Anusavice (ed.), *Dental Materials*, 2003, St. Louis